Supplementary material for paper 1131: Conformal Surface alignment with Optimal Möbius Search

A Experiment Results

In Sec. A.1 and A.2, we provide more results on real data obtained by Möbius Search(MS) and the competitors: Möbius voting (MS), brute force (BF), graph matching (GM) and ICP. In Sec. A.3, we display the numerical values used to plot the bar charts in Fig. 4 (synthetic data results) of the main paper.

A.1 Conformal Teeth Alignment

We chose 5 pairs of teeth and repeat the experiments described in Sec. 5.3 in the main paper. For each pair, we show the qualitative results followed by a table displaying the quantitative results.

A.1.1 Human09 - Human11

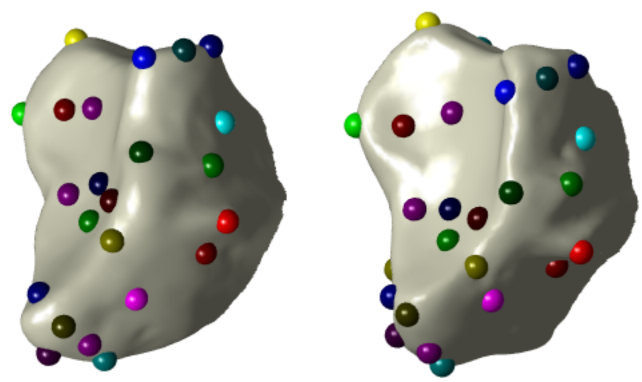

(a) (b)

Figure 1: Correspondences found by MS for Human09 - Human11

		N_1, N_2	Methods	Qbnb	Qmv	Qtruth	Time (sec)
Human09	Human11	100	MS	**40**	**81**	**13**	38.87866
			BF	32	**81**	6	10569.651
			MV	24	60	3	11.18483
			ICP	19	73	7	**0.01788**
		50	MS	**25**	43	**13**	3.16331
			BF	22	**45**	**13**	647.391
			MV	19	30	2	2.17476
			ICP	16	42	12	**0.00811**
		20	MS	**9**	16	**13**	0.36952
			BF	1	**17**	8	17.19584
			MV	3	12	3	0.40676
			GM	2	12	1	39.456
			ICP	1	16	10	**0.00191**

Table 1: Results for conformal alignment of Human09 and Human11

A.1.2 Orangutan 505958 - Orangutan 50960

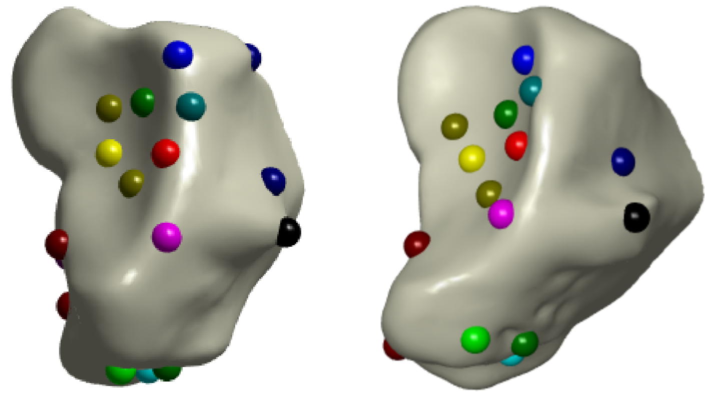

(a) (b)

Figure 2: Correspondences found by MS for Orangutan 505958 - Orangutan 50960

		N_1, N_2	Methods	Qbnb	Qmv	Qtruth	Time (sec)
Orangutan50958	Orangutan50960	100	MS	**40**	76	7	35.966
			BF	29	**78**	**12**	10049.000
			MV	26	61	2	11.283
			ICP	18	46	1	**0.022**
		50	MS	**20**	34	3	2.808
			BF	15	**37**	**12**	649.365
			MV	11	32	1	2.925
			ICP	8	32	1	**0.008**
		20	MS	**9**	12	2	0.297
			BF	2	**17**	4	16.886
			MV	3	11	1	0.541
			GM	2	16	**7**	52.207
			ICP	3	10	2	**0.002**

Table 2: Results for conformal alignment of Orangutan 505958 and Orangutan 50960

A.1.3 V01 - V02

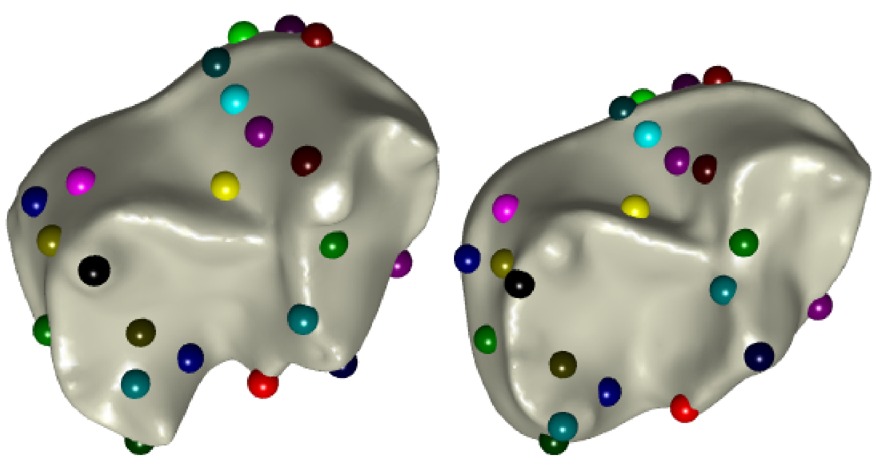

(a) (b)

Figure 3: Correspondences found by MS for V01 - V02

		N_1, N_2	Methods	Qbnb	Qmv	Qtruth	Time (sec)
V01	V02	100	MS	**34**	**81**	**15**	14.691
			BF	25	78	12	10011.000
			MV	14	51	3	2.818
			ICP	21	67	0	**0.023**
		50	MS	**16**	**44**	**13**	2.816
			BF	7	**44**	12	639.578
			MV	5	32	6	3.639
			ICP	8	38	0	**0.006**
		20	MS	**8**	**19**	**15**	0.524
			BF	4	**19**	14	17.039
			MV	0	14	5	1.211
			GM	3	7	1	59.338
			ICP	6	15	1	**0.002**

Table 3: Results for conformal alignment of V01 and V02

A.1.4 Bonobo 38018 - Bonobo 38019

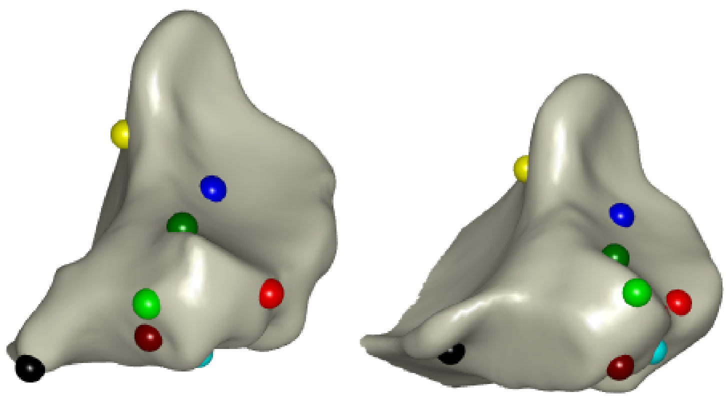

(a) (b)

Figure 4: Correspondences found by MS for Bonobo 38018 - Bonobo 38019

		N_1, N_2	Methods	Qbnb	Qmv	Qtruth	Time (sec)
Bonobo 38018	Bonobo38019	100	MS	**70**	62	**10**	10.971
			BF	45	**68**	0	10025.551
			MV	60	58	6	11.342
			ICP	28	27	1	**0.020**
		50	MS	**17**	33	**5**	6.509
			BF	7	**34**	**5**	633.254
			MV	1	29	2	6.602
			ICP	2	28	2	**0.028**
		20	MS	**5**	13	2	0.624
			BF	0	**15**	**6**	17.550
			MV	2	8	0	0.993
			GM	**5**	7	2	0.001
			ICP	3	10	2	**0.002**

Table 4: Results for conformal alignment of Bonobo38018 and Bonobo38019

A.1.5 x03 - x04

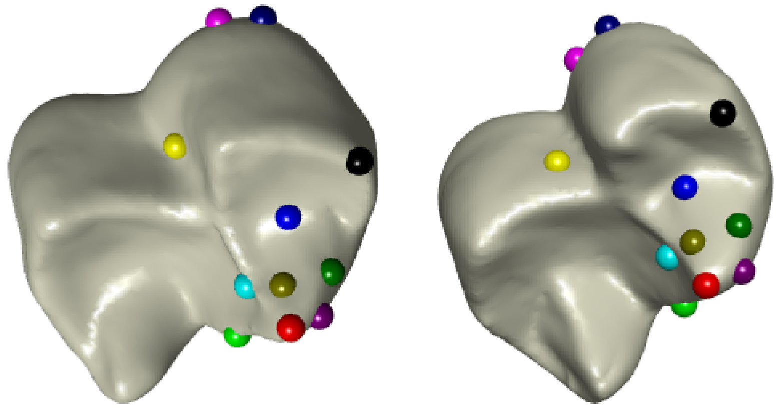

(a) (b)

Figure 5: Correspondences found by MS for x03-x04

		N_1, N_2	Methods	Qbnb	Qmv	Qtruth	Time (sec)
x03	x04	100	MS	**16**	**78**	**14**	30.074
			BF	3	**78**	**14**	10903.700
			MV	7	66	0	42.472
			ICP	5	73	2	**0.021**
		50	MS	**21**	**43**	**16**	4.207
			BF	16	**43**	15	621.235
			MV	12	27	2	2.181
			ICP	9	34	2	**0.005**
		20	MS	**8**	15	**13**	0.638
			BF	3	16	0	18.320
			MV	2	13	1	0.336
			GM	0	14	0	52.530
			ICP	3	**17**	4	**0.002**

Table 5: Results for conformal alignment of x03 and x04

A.2 Conformal Face Alignment

Similar to A.1, the experiments are repeated for 5 more pairs of face.

A.2.1 F0015_FE01WH - F0015_FE02WH

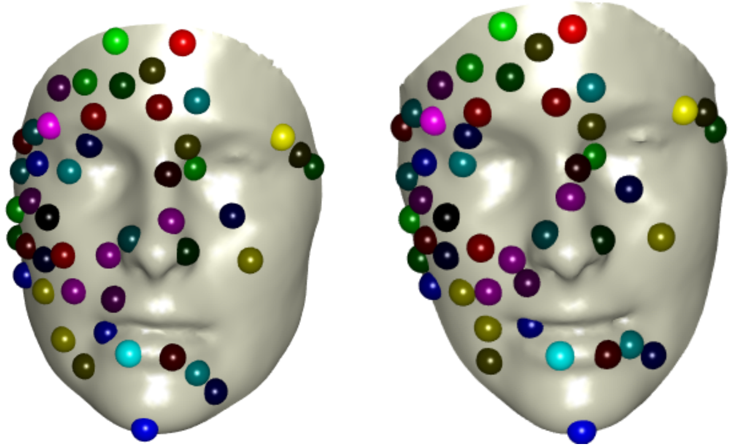

(a) (b)

Figure 6: Correspondences found by MS for F0015_FE01WH - F0015_FE02WH

		N_1, N_2	Methods	Qbnb	Qmv	Qtruth	Time (sec)
F0015_FE01WH	F0015_FE02WH	100	MS	**54**	82	**13**	15.661
			BF	42	**84**	**13**	9982.935
			MV	36	28	1	16.914
			ICP	30	58	0	**0.083**
		50	MS	**24**	40	**13**	4.088
			BF	12	**41**	1	612.245
			MV	7	35	11	1.495
			ICP	10	29	0	**0.005**
		20	MS	**14**	17	**13**	0.710
			BF	10	**18**	11	16.798
			MV	2	10	6	0.138
			GM	12	**18**	12	44.208
			ICP	4	13	0	**0.004**

Table 6: Results for conformal alignment of F0015_FE01WH - F0015_FE02WH

A.2.2 F0049_SU01WH - F0049_SU03WH

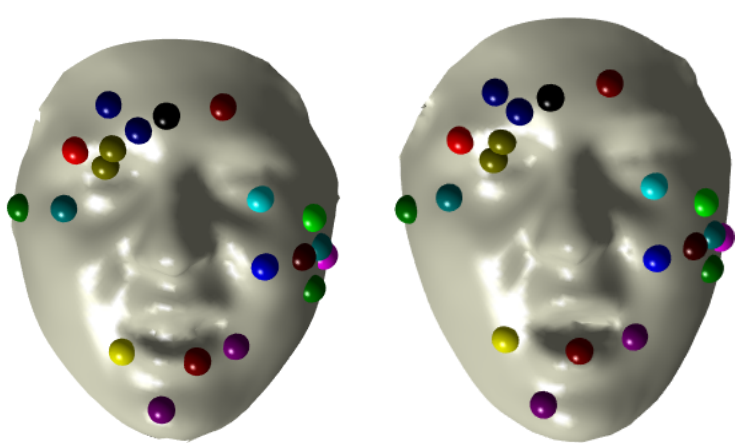

(a) (b)

Figure 7: Correspondences found by MS for F0049_SU01WH - F0049_SU03WH

		N_1, N_2	Methods	Qbnb	Qmv	Qtruth	Time (sec)
F0049_SU01WH	F0049_SU03WH	100	MS	**51**	84	**13**	15.581
			BF	46	**85**	**13**	10011.218
			MV	38	24	0	28.224
			ICP	36	67	0	**0.023**
		50	MS	**29**	44	**13**	4.249
			BF	23	**47**	**13**	635.322
			MV	15	8	1	2.232
			ICP	7	33	0	**0.007**
		20	MS	**13**	**19**	**13**	0.378
			BF	12	**19**	**13**	16.992
			MV	3	7	2	0.693
			GM	2	16	8	66.848
			ICP	2	14	0	**0.003**

Table 7: Results for conformal alignment of F0049_SU01WH and F0049_SU03WH

A.2.3 M0015_HA02WH - M0015_HA04WH

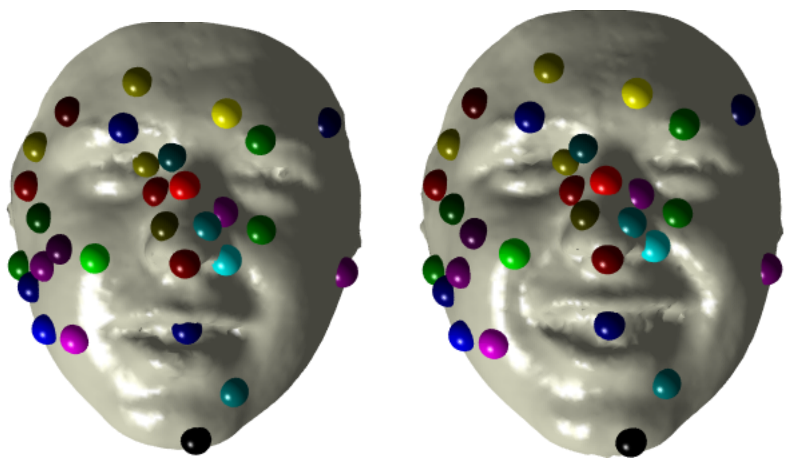

(a) (b)

Figure 8: Correspondences found by MS for M0015_HA02WH - M0015_HA04WH

		N_1, N_2	Methods	Qbnb	Qmv	Qtruth	Time (sec)
M0015_HA02WH	M0015_HA04WH	100	MS	**34**	80	**13**	16.143
			BF	28	**84**	**13**	11992.847
			MV	24	26	1	6.527
			ICP	21	79	12	**0.045**
		50	MS	**17**	42	**13**	10.316
			BF	11	**44**	**13**	648.235
			MV	6	11	2	1.506
			ICP	10	38	**13**	**0.026**
		20	MS	**10**	15	**13**	0.523
			BF	1	**17**	5	18.740
			MV	3	15	**13**	0.326
			GM	3	14	8	86.483
			ICP	6	15	**13**	**0.019**

Table 8: Results for conformal alignment of M0015_HA02WH and M0015_HA04WH

A.2.4 M0040_SA02WH - M0040_SA04WH

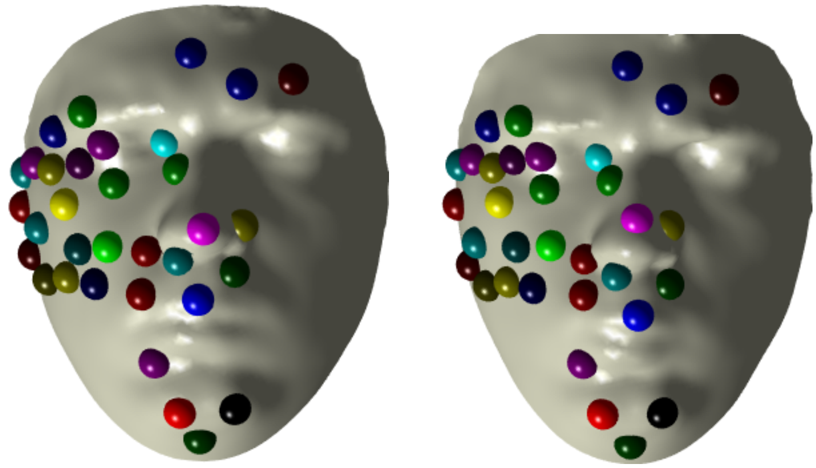

(a) (b)

Figure 9: Correspondences found by MS for M0040_SA02WH - M0040_SA04WH

		N_1, N_2	Methods	Qbnb	Qmv	Qtruth	Time (sec)
M0040_SA02WH	M0040_SA04WH	100	MS	**38**	84	12	14.568
			BF	30	**85**	**13**	10985.872
			MV	23	11	1	14.105
			ICP	18	79	11	**0.232**
		50	MS	**17**	43	12	14.977
			BF	14	**45**	**13**	629.110
			MV	4	17	2	0.767
			ICP	1	42	10	**0.009**
		20	MS	**12**	18	**13**	0.914
			BF	4	**19**	12	16.956
			MV	2	17	12	0.137
			GM	3	17	**13**	29.429
			ICP	3	16	12	**0.002**

Table 9: Results for conformal alignment of M0040_SA02WH and M0040_SA04WH

A.2.5 F0036_AN02AE - F0036_AN02AE

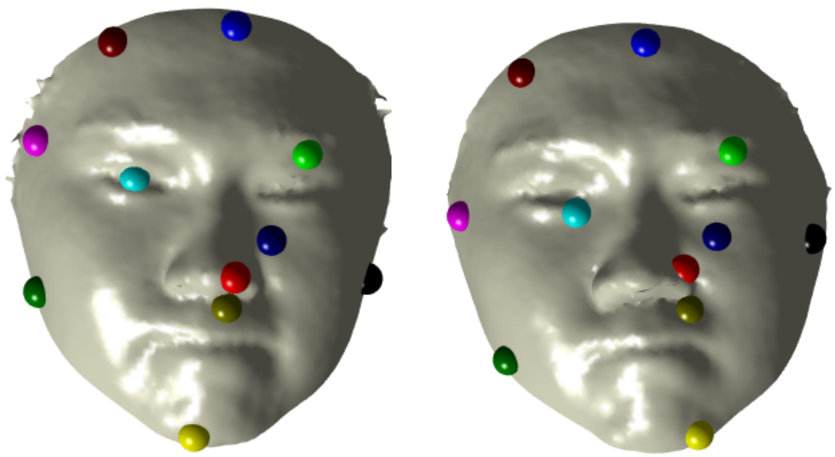

(a) (b)

Figure 10: Correspondences found by MS for F0036_AN02AE - F0036_AN02AE

		N_1, N_2	Methods	Qbnb	Qmv	Qtruth	Time (sec)
F0036_AN02AE	F0036_AN04AE	100	MS	**24**	77	**11**	54.420
			BF	19	**84**	0	10565.549
			MV	10	43	1	2.822
			ICP	8	68	1	**0.024**
		50	MS	**19**	40	6	4.336
			BF	14	**42**	**11**	631.845
			MV	8	8	1	1.484
			ICP	12	37	1	**0.007**
		20	MS	**10**	15	**13**	0.526
			BF	1	**17**	1	16.937
			MV	2	9	2	0.187
			GM	1	14	11	36.986
			ICP	0	14	1	**0.002**

Table 10: Results for conformal alignment of F0036_AN02AE and F0036_AN02AE

A.3 Numerical results for synthetic data

N_1	ρ (%)	Methods	Qbnb	Qmv	Time(sec)
100	0	MS	**100**	71	0.385
		MV	**100**	71	2.557
		BF	**100**	71	11304.600
		ICP	4	40	**0.028**
		ICP2	77	**83**	0.033
	25	MS	**75**	59	1.130
		MV	**75**	59	11.435
		BF	**75**	59	11404.700
		ICP	5	40	**0.021**
		ICP2	48	**72**	0.025
	50	MS	**50**	45	2.569
		MV	0	51	14.141
		BF	0	49	10121.000
		ICP	4	46	0.052
		ICP2	3	**60**	**0.030**

Table 11: Numerical results for synthetic data with $N_1 = 100$

N_1	ρ (%)	Methods	Qbnb	Qmv	Time(sec)
50	0	MS	**50**	**42**	0.072
		MV	**50**	**42**	0.815
		BF	**50**	**42**	618.759
		ICP	2	14	0.010
		ICP2	21	**42**	**0.008**
	25	MS	**37**	**36**	3.339
		MV	**37**	**36**	0.755
		BF	**37**	**36**	642.490
		ICP	1	19	0.021
		ICP2	1	**36**	**0.010**
	50	MS	**25**	25	23.175
		MV	6	6	0.728
		BF	4	4	643.603
		ICP	0	24	0.021
		ICP2	4	**29**	**0.008**

Table 12: Numerical results for synthetic data with $N_1 = 50$

N_1	ρ (%)	Methods	Qbnb	Qmv	Time(sec)
20	0	MS	**20**	**19**	0.15343
		MV	**20**	**19**	0.1365
		BF	**20**	**19**	17.07308
		ICP	1	8	**0.00664**
		ICP2	14	**19**	0.00808
		GM	**20**	**19**	29.281
	25	MS	**15**	**14**	0.16772
		MV	**15**	**14**	0.1965
		BF	**15**	**14**	16.86983
		ICP	1	7	0.01413
		ICP2	1	9	**0.00213**
		GM	**15**	**14**	24.4612
	50	MS	**10**	11	0.38881
		MV	1	11	0.3723
		BF	0	**13**	17.02
		ICP	0	10	0.01533
		ICP2	0	**13**	**0.00182**
		GM	0	4	37.9

Table 13: Numerical results for synthetic data with $N_1 = 20$

B Calculating range limit

B.1 Range limit for solving rotation angle

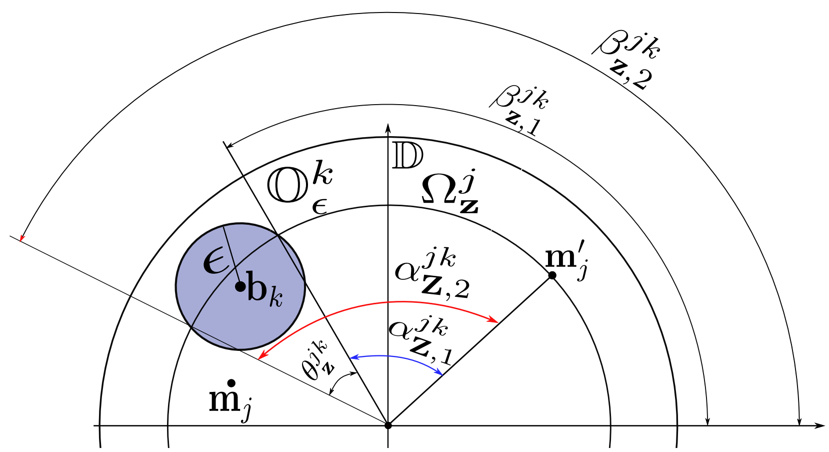

Figure 11: Computing range limits for solving rotation angle

This section explains how the range limit $[\alpha^{jk}_{\mathbf{z},1}, \alpha^{jk}_{\mathbf{z},2}]$ defined in section 3 can be derived.

Let $\theta^{jk}_{\mathbf{z}}$ be the intersection angle between $\Omega^j_{\mathbf{z}}$ and $\mathbb{O}^k_\epsilon$ as depicted in Fig. 11. This angle can be evaluated easily using circle to circle intersection.

Define $\beta^{jk}_{\mathbf{z},1}$ and $\beta^{jk}_{\mathbf{z},2}$ to be the limiting angles of the intersection arc, which can be determined by:

$$\beta^{jk}_{\mathbf{z},1} = \angle \mathbf{b}_k - \frac{\theta^{jk}_{\mathbf{z}}}{2} \tag{1}$$

and

$$\beta^{jk}_{\mathbf{z},2} = \angle \mathbf{b}_k + \frac{\theta^{jk}_{\mathbf{z}}}{2} \tag{2}$$

As can easily be seen, the formula for the range limit $[\alpha^{jk}_{\mathbf{z},1}, \alpha^{jk}_{\mathbf{z},2}]$ will be:

$$\alpha^{jk}_{\mathbf{z},1} = \beta^{jk}_{\mathbf{z},1} - \angle \mathbf{m}'_j \tag{3}$$

and

$$\alpha^{jk}_{\mathbf{z},2} = \beta^{jk}_{\mathbf{z},2} - \angle \mathbf{m}'_j \tag{4}$$

B.2 Range limit for computing upper bound

This section details the steps to compute the range limit $[\alpha^{jk}_{\mathbb{R},1}, \alpha^{jk}_{\mathbb{R},1}]$ defined in bound calculation part in section 4.2 (cf. the main paper).

Let $\theta^{jk}_{\mathbb{R}}$ be the intersection angle between $\Omega^j_{\mathbb{R}}$ and the disk $\mathbb{O}^k_\epsilon$. The way to compute this angle depends on the relative position between $\mathbf{b}_k$ and the annulus $\Omega^j_{\mathbb{R}}$ plus the value of ϵ. Specifically,

C1 If $r^j_{\mathbb{R},1} \leq \sqrt{|\mathbf{b}_k|^2 - \epsilon^2} \leq r^j_{\mathbb{R},2}$ (Fig. 12): $\theta^{jk}_{\mathbb{R}}$ is the angle between two tangent lines starting from the center of the $\mathbb{O}^k_\epsilon$ disk. Mathematically,

$$\theta^{jk}_{\mathbb{R}} = 2 * \arcsin \frac{\epsilon}{|\mathbf{b}_k|} \tag{5}$$

C2 If $\sqrt{|\mathbf{b}_k|^2 - \epsilon^2} < r^j_{\mathbb{R},1}$ or $\sqrt{|\mathbf{b}_k|^2 - \epsilon^2} > r^j_{\mathbb{R},2}$. There are two possibilities:

C2.1 The outline of $\mathbb{O}^k_\epsilon$ intersects with either the inner **or** the outer ring of $\Omega^j_{\mathbb{R}}$: $\theta^{jk}_{\mathbb{R}}$ is computed using circle to circle intersection (Fig. 13)

C2.2 The outline of $\mathbb{O}^k_\epsilon$ intersects with both the inner **and** the outer ring of $\Omega^j_{\mathbb{R}}$: $\theta^{jk}_{\mathbb{R}}$ is determined by the ring that has larger intersection angle with $\mathbb{O}^k_\epsilon$ using circle to circle intersection (Fig. 14)

Similar to B.1, define $\beta^{jk}_{\mathbb{R},1}$ and $\beta^{jk}_{\mathbb{R},2}$ to be the limiting angles of the intersection area

$$\beta^{jk}_{\mathbb{R},1} = \angle \mathbf{b}_k - \frac{\theta^{jk}_{\mathbb{R}}}{2} \tag{6}$$

and

$$\beta^{jk}_{\mathbb{R},2} = \angle \mathbf{b}_k + \frac{\theta^{jk}_{\mathbb{R}}}{2} \tag{7}$$

Finally, the range limit can be computed as:

$$\alpha^{jk}_{\mathbb{R},1} = \beta^{jk}_{\mathbb{R},1} - \theta^j_{\mathbb{R},2} \tag{8}$$

and

$$\alpha^{jk}_{\mathbb{R},2} = \beta^{jk}_{\mathbb{R},2} - \theta^j_{\mathbb{R},1} \tag{9}$$

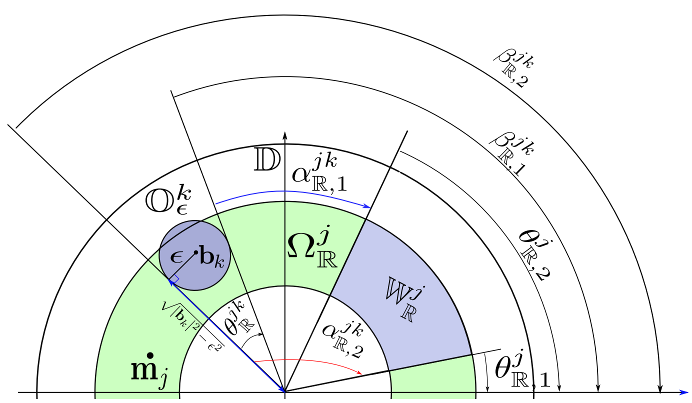

Figure 12: Illustration of C1: $r^j_{\mathbb{R},1} \leq \sqrt{|\mathbf{b}_k|^2 - \epsilon^2} \leq r^j_{\mathbb{R},2}$

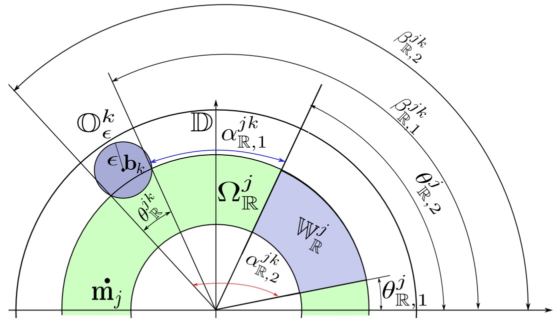

(a) Outline of $\mathbb{O}^k_\epsilon$ intersects with the outer ring of $\Omega^j_{\mathbb{R}}$

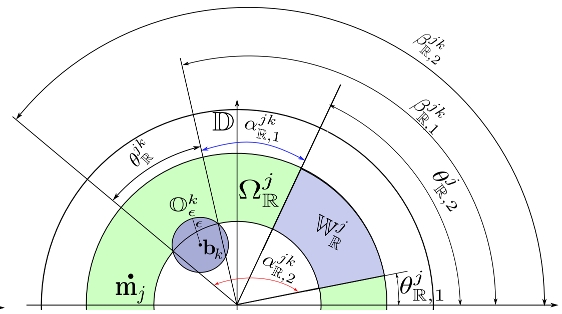

(b) Outline of $\mathbb{O}^k_\epsilon$ intersects with the inner ring of $\Omega^j_{\mathbb{R}}$

Figure 13: Illustration of C2.1: Outline of $\mathbb{O}^k_\epsilon$ intersects with either the inner or outer ring of the annulus $\Omega^j_{\mathbb{R}}$

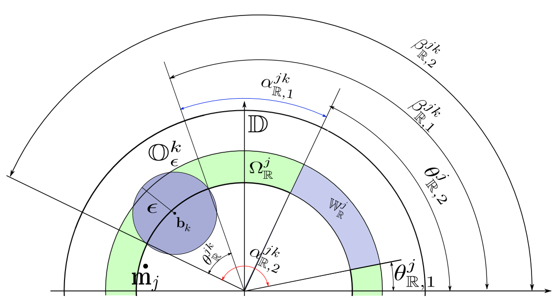

(a) $\theta^{jk}_{\mathbb{R}}$ is determined by intersection between the outline of $\mathbb{O}^k_\epsilon$ with the inner ring

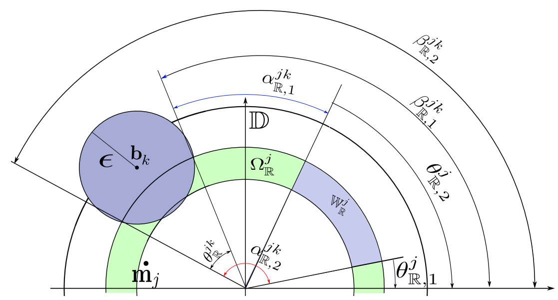

(b) $\theta^{jk}_{\mathbb{R}}$ is determined by intersection between the outline of $\mathbb{O}^k_\epsilon$ with the outer ring

Figure 14: Illustration of C2.2: Outline of $\mathbb{O}^k_\epsilon$ intersects with both the inner or outer ring of the annulus $\Omega^j_{\mathbb{R}}$

C Solving for rotation angle

Algorithm 1 in this document gives the method for solving problem (12) in Sec. 3 of the main paper, i.e., finding the rotation angle that intersects the highest number of angular ranges $\mathcal{S}^j_{\mathbf{z}} = \left\{[\alpha^{jk}_{\mathbf{z},1}, \alpha^{jk}_{\mathbf{z},2}]\right\}_{k=1}^{N_2}$.

This algorithm runs very efficiently in $\mathcal{O}(N \log N)$ time. See Chapter 10 of [M. De Berg, M. Van Kreveld, M. Overmars, and O. C. Schwarzkopf. Computational geometry. Springer, 2000] if more details are required.

Algorithm 1 Interval Stabbing

Require: Set of angular ranges $\left\{ \mathcal{S}^j_{\mathbf{z}} = \left\{ [\alpha^{jk}_{\mathbf{z},1}, \alpha^{jk}_{\mathbf{z},2}] \right\}_{k=1}^{N_2} \right\}_{j=1}^{N_1}$

Set $\mathcal{S} \leftarrow$ empty set; $\theta^* \leftarrow$ null; $U(\mathbf{z}) \leftarrow 0$; $l \leftarrow 0$
for all $j = 1 \ldots N_1$ **do**
  for all angular intervals $[\alpha^{jk}_{\mathbf{z},1}, \alpha^{jk}_{\mathbf{z},2}]$ in $\mathcal{S}^j_{\mathbf{z}}$ **do**
    $l \leftarrow l + 1$
    $s_l.a \leftarrow \alpha^{jk}_{\mathbf{z},1}$
    $s_l.f \leftarrow 1$
    Insert s_l into $\mathcal{S}$
    $l \leftarrow l + 1$
    $s_l.a \leftarrow \alpha^{jk}_{\mathbf{z},2}$
    $s_l.f \leftarrow -1$
    Insert s_l into $\mathcal{S}$
  end for
end for
Sort all elements $s_l \in \mathcal{S}$ by $s_l.a$ in ascending order $\rightarrow S'$
$c \leftarrow 0$
for all $s_l \in S'$ **do**
  $c \leftarrow c + s_l.f$
  if $c > U(\mathbf{z})$ **then**
    $\theta^* \leftarrow s_l.a$
    $U(\mathbf{z}) \leftarrow c$
  end if
end for
return θ^* and $U(\mathbf{z})$.